Structural Engineering and Mechanics, *Vol. 47, No. 4 (2013) 575-598*
DOI: http://dx.doi.org/10.12989/sem.2013.47.4.575

Investigation of shear transfer mechanisms in repaired damaged concrete columns strengthened with RC jackets

Achillopoulou D.V.* and Karabinis A.I.[a]

Reinforced Concrete Laboratory, Civil Engineering Department, Polytechnic School, Democritus University of Thrace, Vas. Sofias 12, 67100, Xanthi, Greece

(Received December 20, 2012, Revised July 22, 2013, Accepted July 31, 2013)

Abstract. The study presents the results of an experimental program concerning the shear force transfer between reinforced concrete (RC) jackets and existing columns with damages. In order to investigate the effectiveness of the repair method applied and the contribution of each shear transfer mechanism of the interface. It includes 22 concrete columns (core) (of 24,37MPa concrete strength) with square section (150mm side, 500 mm height and scale 1:2). Ten columns had initial construction damages and twelve were subjected to initial axial load. Sixteen columns have full jacketing at all four faces with 80mm thickness (of 31,7MPa concrete strength) and contain longitudinal bars (of 500MPa nominal strength) and closed stirrups spaced at 25mm, 50mm or 100mm (of 220MPa nominal strength). Fourteen of them contain dowels at the interface between old and new concrete. All columns were subjected to repeated (pseudo-seismic) axial compression with increasing deformation cycles up to failure with or without jacketing. Two load patterns were selected to examine the difference of the behavior of columns. The effects of the initial damages, of the reinforcement of the interface (dowels) and of the confinement generated by the stirrups are investigated through axial- deformation (slip) diagrams and the energy absorbed diagrams. The results indicate that the initial damages affect the total behavior of the column and the capacity of the interface to shear mechanisms and to slip: a) the maximum bearing load of old column is decreased affecting at the same time the loading capacity of the jacketed element, b) suitable repair of initially damaged specimens increases the capacity of the jacketed column to transfer load through the interface.

Keywords: concrete jacket; initial damage; force transfer; repair and strengthening

1. Introduction

Nowadays, a large number of Reinforced Concrete (R.C.) structures need interventions which concern either repairing or/ and strengthening of the critical structural elements such as columns especially after construction damages or overloading (seismic) damages. The common reasons of interventions are: a) damages to the critical elements (columns) due to high levels of loading (ex. earthquake), b) initial construction damages (incomplete consolidation of concrete during concreting), c) the need to improve the whole capacity of the structure especially in those designed and constructed with older seismic codes, d) the need to increase the bearing capacity due to

*Corresponding author, Ph.D. Student, E-mail: dimiachi@civil.duth.gr
[a]Professor, E-mail: karabin@civil.duth.gr

http://www.techno-press.org/?journal=sem&subpage=8 ISSN: 1225-4568 (Print), 1598-6217 (Online)

different use of the structure itself or due to superposition of a store. In light of modern seismic codes, these structures are often characterized as inadequate or of increased seismic hazard, especially in high seismicity regions where a future major seismic event is more expected notably when they are already pre-loaded beyond strength limits. Thus, the necessity of reliable retrofit of these structures arises. Retrofitting strategies are guided by the fact that as well as repairing usually it is required higher level of strength and ductility of structural elements. During last decades jacketing of columns through R.C. is widely applied because it has been proven an efficient method to enhance the load capacity and ductility of element (Fardis (2009), Julio *et al*. (2005), Bousias *et al*. 2004, Spathis *et al*. 2006, Vandoros *et al*. 2006a, b). The efficiency of jacketing depends strongly on the behavior of the interface of old and new concrete and of its capacity in transferring loads. The shear transfer mechanisms are concrete-to-concrete cohesion and friction (aggregate interlock) (Haskett *et al*. 2011, Julio 2005), and dowel action (Ragip *et al*. 2007).

The load transfer between old concrete (core) and new concrete (jacket) has been studied analytically and experimentally thoroughly and suggestions are made about how every mechanism works (Xiao *et al*. 2012, Sim *et al*. 2013, Thermou *et al*. 2011). All these suggestions for the RC jacketing design have been incorporated in various codes world-widely such as FIB (Model Code 2010), and ACI-318R-08 Building Code, European Standard EN 199-8 part 3 (GRC: Greek Retrofit Code attuned (Table 1). The codes contain semi-empirical relations with which it's possible to design the jacketing and calculate the basic values of the individual components of the load transfer from old to new concrete. Nevertheless, parameters such as initial loading or damage to the old column (core) or the kind and way of loading (monotonically, repeatedly, cyclic, directly or indirectly through core and its transverse reinforcement) mostly beyond design deformations (slip) are not defined. All these parameters are considered critical for beyond the design loads behavior of the retrofitted and jacketed column. These parameters are investigated separately or in combination in this paper. In real structures columns are also subjected to vertical forces (earthquake). In this paper only the parameters of shear transfer mechanisms examined. For those reasons the specimens were subjected to axial compression only. The experimental program held at the Reinforced Concrete Lab at Democritus University of Thrace (D.U.Th.) and in this phase includes 22 specimens. They contain different percentages of transverse reinforcement at core and jacket, providing different mean normal stress at the interface. The different treatment of the interface between old and new concrete such as the different kind of cohesion developed is tested (ex. due to coating with synthetic polymer sheets).Also, the factor of possible initial damage due to construction imperfections that is not referred and analyzed extensively in the various codes that affects the efficiency of the repair is examined (Achillopoulou *et al*. 2012). Damage indices are proposed to quantify the extension of the damage in a quick and simplified way.

2. Shear transfer mechanisms

In an RC element strengthened with jacket the basic load transfer mechanisms between core and jacket are: a) concrete to concrete cohesion (aggregate interlock), b) friction (attributed to the clamping action of the stirrup legs normal to the interface) and c) dowel action.

During last decades research on load transferring is directed primarily to the examination of the retrofitted element but not the interface. World-widely codes suggest relations and values considering the interface (*FIB* (Model Code 2010, bulletin 55), and ACI-318R-08 Building Code, European Standard EN 199-8 part 3 (GRC: Greek Retrofit Code attuned) (Table 1)).

Table 1 Load transfer mechanisms in codes

Load Transfer Mechanisms on Concrete Interfaces					
	Cohesion		Friction	Dowel Action	
	Shear stress (1)		μ: friction coefficient (3)	Shear stress	
FIB (Model Code 2010, bulletin 55)	~1.5-2.5 N/mm^2 rough interface ~2.5-3.5 N/mm^2 very rough interface ~1.5-2.0 N/mm^2 high pressure jetting (interlock)		0.5-0.7: smooth interface 0.7-1.0: rough interface 1.0-1.4: very rough interface	Cohesion+ interlock+ friction+ dowel: $\tau_{u,1} = \tau_c + \mu \cdot (\sigma + \kappa \cdot \rho \cdot f_y)$ (7) $\kappa = \frac{\sigma_s}{f_y} \leq 1$: coefficient of interaction Force of one dowel bar: $F_s = k \cdot A_s \cdot \sqrt{f_{cc}}\sqrt{f_y}\left(s/s_{max}\right)^{0,5}$ (8) s_{max}= *0.10-0.20*d_s Total: $\tau_{u,1} = \tau_c + \mu \cdot (\sigma + \kappa \cdot \rho \cdot f_y) + \alpha \cdot \rho\sqrt{f_{cc}f_y} \leq \beta \cdot v\, f_{cc}$ (9) α: interaction coefficient	
ACI-318R-08 Building Code	μ: friction coefficient (4)			Shear force	
	1.4λ: monolithic element 1.0λ: designed rough 0.6λ: rough 0.7λ: dowel presence λ: 1.00 regular concrete, λ: 0.75 high strength concrete			$V_n = A_{vf} \cdot f_y \cdot (\mu \cdot sina + cosa)$ (10) α: inclination of reinforcement crossing the interface	
	Shear stress (2)	slip	Shear stress (5)	Slip (6)	Shear stress
EN1998-3 (Greek Retrofit Code)	$0.25 \cdot f_{ct}$ smooth interface $0.75 \cdot f_{ct}$ rough interface $1.00 \cdot f_{ct}$ strong connective material/pressure/shotcrete	0.01-0.02mm	$\tau_{fud} = \mu \cdot \sigma_0$ smooth interface $\tau_{fud} = 0.4 \cdot \left(f_{cd}^2 \cdot \sigma_{cd}\right)^{1/3}$ Rough interface	$s_{fu} = 0.15 \cdot \sqrt{\sigma_{cd}}$ $s_{fu} = 2mm$	Clamp: $\tau_{fRd} = \mu \cdot (\rho \cdot f_{yd} + \sigma_{cd}) < 0.3 \cdot f_{cd}$ (11) Force of one dowel bar: $F_{ud} = 1.3 \cdot d_b^2\sqrt{f_{cd}f_{yd}} \leq A_s f_{yd}/\sqrt{3}$ (12)

2.1 Cohesion

The concrete-to-concrete cohesion depends on the kind of the interface (Xiao *et al*. 2013, Julio *et al*. 2005). Each regulation depending on the treatment of the interface (smooth, rough, very rough, high pressure, jetting, shotcrete, etc.) provide different values of cohesion. *FIB* considers a lower and an upper limit for cohesion but has no provision for smooth interfaces (Table 1, Eq. (1)). ACI does not consider cohesion at all for every kind of interface. Finally, EN 1998 part 3- GRC in contrast, correlates cohesion with the tensile strength of the wicker concrete between core and jacket. For smooth interface according to EN 1998 part 3- GRC the shear stress due to cohesion is $\tau = 0{,}25 \cdot f_{ct}$ (Fig. 1, Table 1, Eq. (2)). Also, only EN 1998 part 3- GRC provides values of slip for the loss of cohesion, that is $s = 0{,}01 - 0{,}02\ mm$.

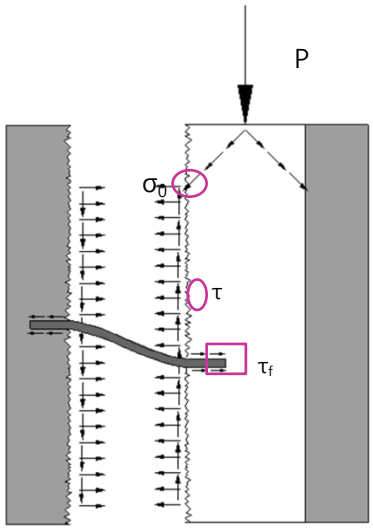

Fig. 1 Shear transfer mechanisms on concrete interfaces

2.2 Friction

The load transfer through friction depends only on the friction coefficient (μ) and the normal stress applied at the interface. FIB again considers a lower and an upper limit of friction coefficient for every kind of interface (rough, very rough, etc.) (Table 1, Eq. (3)). Also, for smooth interface provides values of μ between 0.5 and 0.7 for the friction coefficient.) (Table 1, Eq. (4)). ACI considers the friction coefficient correlated with the presence of dowels and the kind of concrete through coefficient λ (1.4λ: monolithic element, 1.0λ: designed rough, 0.6λ: rough, 0.7λ: dowel presence, values of λ: 1.00 for regular concrete, λ: 0.75 for high strength concrete). EN 1998 part 3- GRC considers friction for smooth and rough interface differently (Table 1, Eq. (5)). The friction coefficient μ for smooth interface is considered 0.4. Again, EN 1998 part 3- GRC provides provision of slip beyond which friction is lost, $s_{fu} = 0{,}15 \cdot \sqrt{\sigma_{cd}}$ (Table 1, Eq. (6)).

2.3 Dowel action

As far as dowel action is considered, all codes consider the shear stress of dowels in the same way. Finally, the force of one dowel bar is differently defined. Fib correlates it with coefficients of interaction and the slip of one dowel bar and the cylinder compressive uniaxial stress of concrete, $F_s = k \cdot A_s \cdot \sqrt{f_{cc}}\sqrt{f_y}\left(s/s_{max}\right)^{0,5}$ (Table 1, Eq. (8)). ACI takes into consideration the inclination of the dowel bars crossing the interface $V_n = A_{vf} \cdot f_y \cdot (\mu \cdot sina + cosa)$ (Table 1, Eq. (10)) and finally EN 1998 part 3- GRC only correlates it with the size of the dowel bar d_b, $F_{ud} = 1{,}3 \cdot d_b^2\sqrt{f_{cd} f_{yd}} \leq A_s f_{yd}/\sqrt{3}$ (Table1, Eq. (12)).

It is noted that all these codes do not take into consideration possible damages, initial (construction) or overloading.

It is obvious that even though all these three codes accept the fundamental load transfer mechanisms through interfaces of old and new concrete, nevertheless the limits of application and

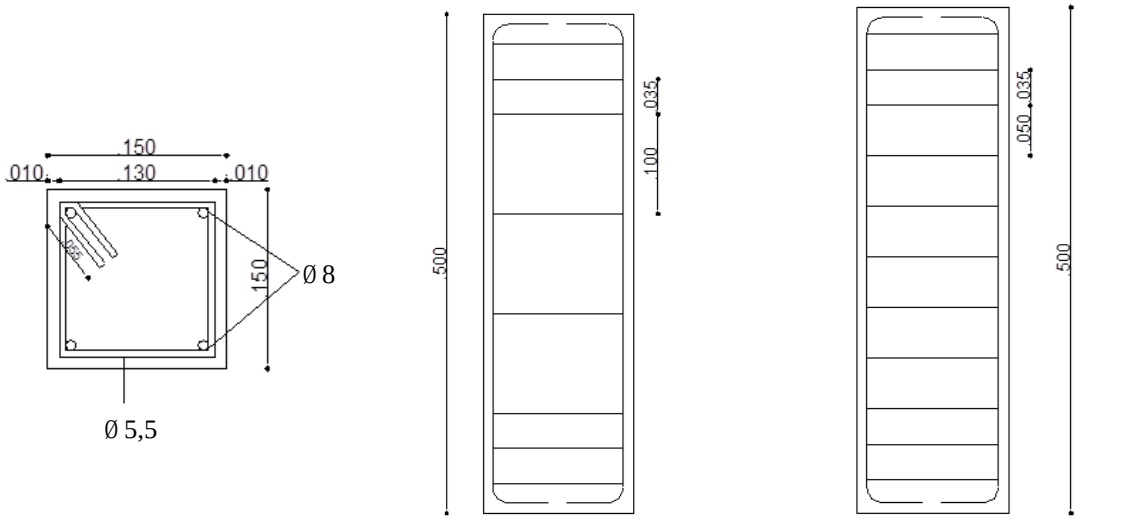

(a) Square section (mm) (b) ω_{wc}=0.075 (mm) (c) ω_{wc}=0.15 (mm)

Fig. 2 Section and transverse reinforcement of columns

consequently the results of design of intervention in an RC element with jackets, differ, depending on each used code.

3. Experimental investigation

3.1 Old columns (Cores)

The experimental investigation includes results of 22 columns of square section with 150 mm width and 500 mm height in scale 1:2 (typical column used in real structures) (Fig. 12(a)). In the considered old columns (cores) concrete of 24.37MPa strength was used (cylinder specimens of 300mm height and 150mm diameter were tested to define the concrete strength), commonly used in building structures in the last decades and 32mm maximum size of aggregate. Four columns were made of plain concrete (UR). The rest include four longitudinal steel bars of 8mm diameter (500MPa nominal strength), that is the minimum volumetric ratio defined by old and new codes (ρ=1%). Seven columns contain closed stirrups spaced at 100mm (mechanical ratio of transverse reinforcement: ω_{wc}=0.075, 220MPa nominal strength, measured yield stress through tension tests f_y=250.76 MPa) and eleven with 50mm stirrup spacing (ω_{wc}=0.15), all adequately anchored (Fig. 2(b), (c)). The selection of the reinforcement was made according to the minimum percentage of longitudinal reinforcement (approximately 1%) and to low and medium transverse reinforcement ratios as practiced in structures with no high ductility requirements. Also, the diameters were selected in order to avoid any possible scale phenomena.

3.2 Damages

The core damages refer to: a) construction damages, b) pre- loading damages.

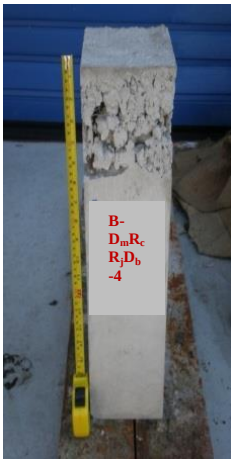

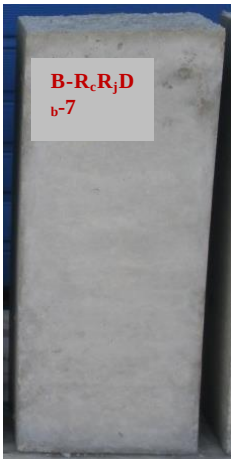

(a) Specimen with construction (initial) damages (b) Specimen without damages (B-$R_cR_jD_b$-7)

Fig. 3 View of specimens

(a) (b)

Fig. 4 (a) Structural initial damages of specimen B-$D_mR_cR_jD_b$-4 (b) Structural initial damages of specimen B-$D_mR_cR_jD_b$-5

The size of aggregate in combination with poor consolidation of concrete led to initial construction damages in nine columns (Fig. 3(a), Fig. 4). Those damages are usually observed in columns of old type buildings. Twelve columns were subjected to axial compression in order to create damages due to overloading (pre- loading). The pre-loading (of cores) axial load was applied monotonically (Specimens: B-$R_cR_jD_b$-6, B-$R_cR_jD_b$-7) or repeatedly (Specimens: B-$D_mR_cR_j$-3, B-$D_mR_cR_jD_b$-4, B-$D_mR_cR_jD_b$-5, A-$D_mR_cR_jD_b$-2). The monotonic loading ended after the maximum load was reached, while the repeating pre-loading continued to a decreasing branch (Fig. 5).

Before testing the damaged columns (cores) were repaired with high strength thixotropic type

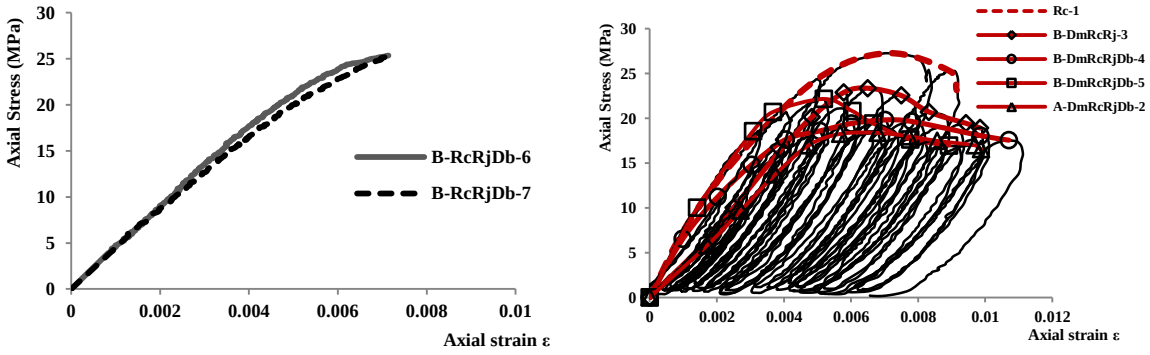

(a) (b)

Fig. 5 (a) Monotonic pre-loading (before jacketing): axial stress vs strain diagram of cores (b) Repeated pre-loading (before jacketing): axial stress vs strain diagram of cores

Fig. 6 Experimental setup

concrete. Nine columns were subjected to initial loading (pre-loading), two of them without construction damages. Specimens B-$R_cR_jD_b$-6 and B-$R_cR_jD_b$-7 were subjected to axial loading monotonically to maximum axial strain ($\varepsilon_{pr\text{-}lmax}$=6‰) before jacketing (Fig. 5(a)), while specimens B-$D_mR_cR_j$-3, B-$D_mR_cR_jD_b$-4, B-$D_mR_cR_jD_b$-5 and A-$D_mR_cR_jD_b$-2 were subjected to pre-loading repeatedly at maximum axial strain $\varepsilon_{pr\text{-}l}$= 10‰ that corresponds to the 85% of the maximum load (cycles of 0.5‰ axial strain) (Fig. 4(b)). The axial loading is applied in a compression machine with a capacity of maximum load 3000 KN (Fig. (6)). The deformations of the column come out from the measurement of the relative displacements between the two loading platens with the use of Displacement Transducers (DT). The specimen details are included in Table 2.

3.3 Retrofit procedure

Fifteen columns were strengthened with RC jacket of 80 mm thickness (total dimension of width: 310 mm) of high strength concrete (nominal compression strength: f_c=31.52 MPa, maximum aggregate: d_{AGR}=8 mm).

In ten columns 6 dowels of 10 mm diameter were placed (Fig. 7(a)) with injected cementitious grout of very small particle size and thixotropic consistency (steady expansion grout), (Sika

Table 2 Details of specimens

Specimen	Dowels	Longitudinal Reinforc-ement (Core/Jacket)	Transverse Reinf-orcement		Repair of Core with Initial (str-uctural) damage (EMACO)	Coating of Inte-rface	Pre- Loading of Core
			Core ω_{wc}	Jacket ω_{wj}			
UR-1	-	-/(not jacketed)	-	-	-	-	-
R_c-1	-	4Ø 8/(not jacketed)	0.15 (Ø 5.5/5)	-	-	-	YES (Repeatedly)
D_mR_c-1	-	4Ø 8/(not jacketed)	0.075 (Ø 5.5/10)	-	√	-	YES
R_c-2	-	4Ø 8/(not jacketed)	0.075 (Ø 5.5/10)	-	-	-	YES
D_mR_c-3	-	4Ø 8/(not jacketed)	0.075 (Ø 5.5/10)	-	√	-	YES
D_mRc-4	-	4Ø 8/(not jacketed)	0.075 (Ø 5.5/10)	-	√	-	YES
D_mRc-5	-	4Ø 8/(not jacketed)	0.15 (Ø 5.5/5)	-	√	-	YES
A-UR-2	-	-	-	-	-	-	-
A-$D_mR_cR_jD_b$-1	6Ø 10	4Ø 8/4Ø 8	0.15 (Ø 5.5/5)	1.86 (Ø 5.5/2,5)	√	RESIN	-
A-$D_mR_cR_jD_b$-2	6Ø 10	4Ø 8/4Ø 8	0.075 (Ø 5.5/10)	0.92 (Ø 5.5/5)	√	RESIN	YES (Repeatedly)
A-$R_cR_jD_b$-3	6Ø 10	4Ø 8/4Ø 8	0.075 (Ø 5.5/10)	0.4 (Ø 5.5/10)	-	-	-
A-$R_cR_jD_b$-4	6Ø 10	4Ø 8/4Ø 8	0.15 (Ø 5.5/5)	0.92 (Ø 5.5/5)	-	POLYMER	-
A-$R_cR_jD_b$-5	6Ø 14	4Ø 8/4Ø 8	0.15 (Ø 5.5/5)	0.92 (Ø 5.5/5)	-	POLYMER	-
B-$R_cR_jD_b$-1	6Ø 14	4Ø 8/4Ø 8	0.15 (Ø 5.5/5)	0.4 (Ø 5.5/10)	-	POLYMER	-
B-$R_cR_jD_b$-2	6Ø 10	4Ø 8/4Ø 8	0.075 (Ø 5.5/10)	0.4 (Ø 5.5/10)	√	POLYMER	-
B-$D_mR_cR_j$-3	-	4Ø 8/4Ø 8	0.15 (Ø 5.5/5)	0.4 (Ø 5.5/10)	√	RESIN	YES (Repeatedly)
B-$D_mR_cR_jD_b$-4	6Ø 10	4Ø 8/4Ø 8	0.15 (Ø 5.5/5)	1.86 (Ø 5.5/2,5)	√	RESIN	YES (Repeatedly)
B-$D_mR_cR_jD_b$-5	6Ø 10	4Ø 8/4Ø 8	0,15 (Ø 5,5/5)	0.92 (Ø 5.5/5)	√	RESIN	YES (Repeatedly)
B-$R_cR_jD_b$-6	6Ø 10	4Ø 8/4Ø 8	0,15 (Ø 5,5/5)	0.92 (Ø 5.5/5)	-	-	YES
B-$R_cR_jD_b$-7	6Ø 10	4Ø 8/4Ø 8	0.15 (Ø 5.5/5)	0.4 (Ø 5.5/10)	-	-	YES
B-UR-3	-	-	-	-	-	-	-
B-URD$_b$-4	6Ø 10	-	-	-	-	-	-

Note:

A: Load Pattern A,
B: Load Pattern B
D_m: damage due to construction imperfections
D_b: dowels

Note:

UR: unreinforced core
UR_j: unreinforced jacket
R_c: reinforced core
R_j: reinforced jacket

Ancorfix3) to connect core and jacket. Dowels were designed according to the minimum percentage of reinforcement normal to the interface per area given by codes. EN 1998 part 3- GRC

(a) Specimen (core) with dowels (B-$D_mR_cR_jD_b$-4)

(b) Specimen coated with synthetic polymer sheet (B-$R_cR_jD_b$-2)

Fig. 7 Preparation of specimens before jacketing

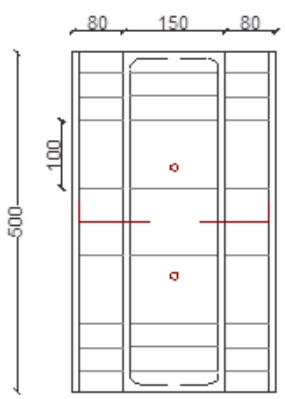

(a) w_c=0.075 - w_j=0.035

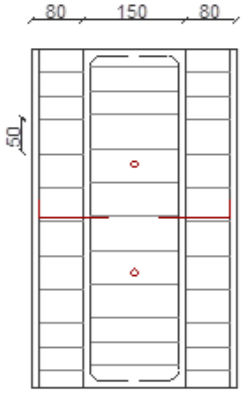

(b) w_c=0.15 - w_j=0.071

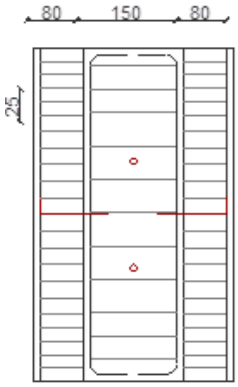

(c) w_c=0.15 - w_j=0.142

Fig. 8 Transverse reinforcement of core and jacket

defines as minimum ratio ρ=1.2‰ but were placed ρ=1.6‰. Five columns were coated with resin of two-component without solvents (Sikadur-32N, LP), so as to achieve adequate adhesion between old and new concrete. Four columns were coated with synthetic polymer sheets so as to minimize the friction forces at the interface (Fig. 7(a)). Finally, one column contain no bars, both core and jacket is made of plain concrete.

The jackets included 4 longitudinal bars of 8 mm diameter and closed stirrups spaced at 25 mm, 50 mm and 100 mm, again of 220 MPa nominal yield stress (measured yield stress through tension tests f_y=250.76 MPa). As shown in Fig. 8, specimens with transverse reinforcement of the jacket at ω_{wj}=0.40 (mechanical percentage of stirrups, normalised at the confined area of the jacket only) contain 8 closed stirrups (n_s) (Fig. 3(a)). Suchlike, specimens with ω_{wj}=0.92 and ω_{wj}=1.86 contain 11 and 21 stirrups respectively. The top and bottom of each specimen contain more stirrups in order to secure that in these regions no damage will take place during test. The jacketed specimens were subjected to axial compression only according to two different Load Patterns (Fig. 9):

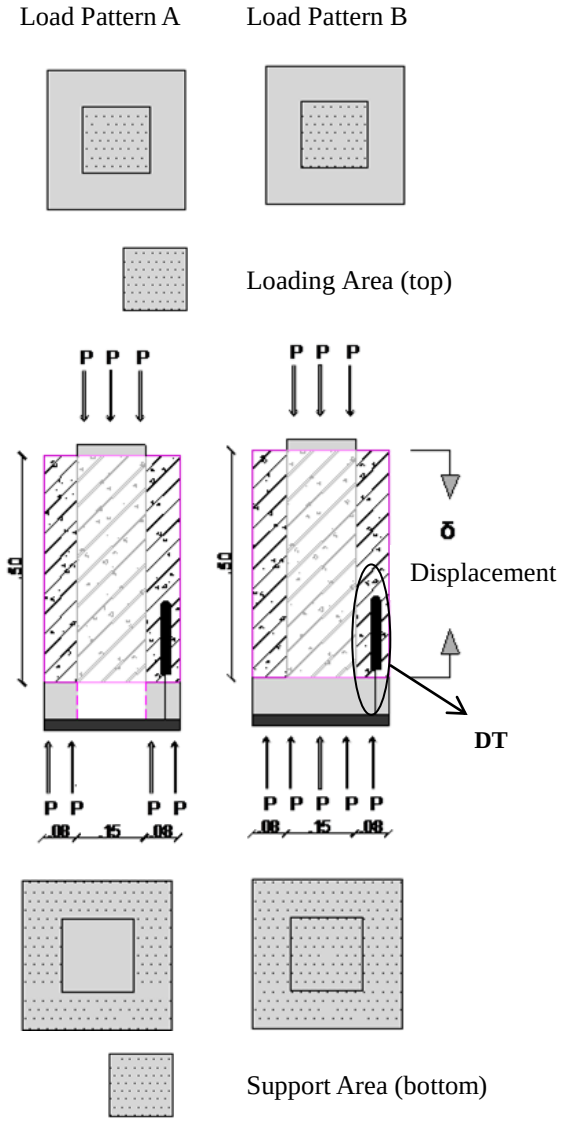

Fig. 9 Shape of load patterns

• Load Pattern A (LPA): Direct loading of old column (core) and support of jacket section only. The purpose is the investigation of load transfer from core (old concrete) to jacket (new concrete) depending on the resistance mechanisms of the interface (cohesion, aggregate interlock, dowels, anchors).

• Load Pattern B (LPB): Direct loading of core with the entire retrofitted element supported. That case simulates the function of a retrofitted column of a real structure where the growth of the axial load takes place through the old column (core). Even if the jacket crosses the beam- column joint, due to the different time of casting, the concrete of the jacket presents shrinkage phenomena. As a result there is a region of the old column not fully jacketed.

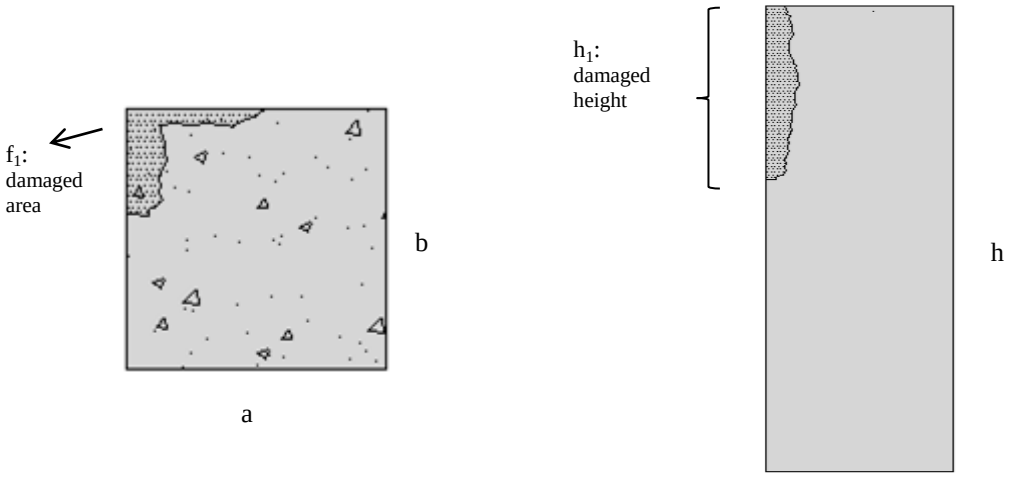

Fig. 10 (a) Section index, (b) Height index

Briefly, the current experimental program considers the following parameters: a. kind of connection of core and jacket: cohesion, epoxy glue, dowels and anchors, b. percentage of transverse reinforcement (stirrups) of core and jacket, c. type of loading- Load Patterns, d. damages of the core (construction or overloading).

4. Experimental results

4.1 Evaluation of construction damages

The construction damages simulate the effect of poor in situ consolidation of concrete with large size of aggregate observed in some cases in columns of old-type building. Construction damages are used to examine the effectiveness of repair before jacketing. For these purposes, concrete of nominal strength f_c=24.37MPa with d_{AGR}=32mm was used. The consolidation took place without all the necessary provisions. After removing the formworks the active height and active section of each specimen was calculated (Fig. 10). Finally, the specimens were repaired with high strength thixotropic type concrete before jacketing.

In order to define the percentage of initial construction damage caused to the columns, a damage indicator d_v (Eq. (13)) is adopted. It consists of two individual ones, d_s referring to the penetration of the damage in the section and d_h referring to the expansion of the damage axially.

$$d_v = 1 - [(1 - d_s) \cdot (1 - d_h)] \tag{13}$$

The indicator d_s referring to the section is a percentage of the damaged area (f_1) to the original section area (f_{tot}) (Eq. (13.a)), as shown in Fig. 10(a).

$$d_s = \frac{f_1}{f_{tot}} \tag{13.a}$$

The indicator d_h referring to the height is a percentage of the damaged height (h_1) to the original height (h_{tot}) (Eq. (13.b)), as shown in Fig. 10(b).

Table 3 Damaged indices

Specimen	d_s (%)	d_h (%)	d_v (%)
D_mR_c-1	25	10	31
D_mR_c-3	25	14	33
D_mR_c-4	13	14	24
D_mR_c-5	37	26	50
A-$D_mR_cR_jD_b$-1	25	20	36
A-$D_mR_cR_jD_b$-2	31	14	37
B-$D_mR_cR_j$-3	13	24	34
B-$D_mR_cR_jD_b$-4	25	28	41
B-$D_mR_cR_jD_b$-5	31	22	41

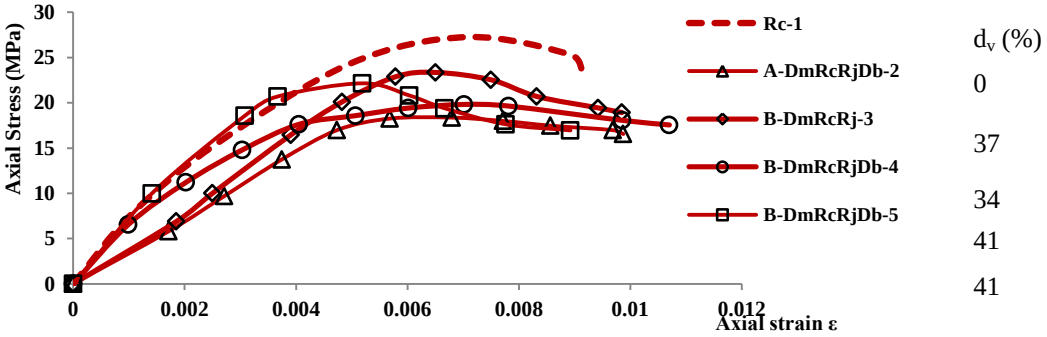

Fig. 11 Envelopes of axial stress- axial strain diagram of specimens subjected to repeated pre-loading with different percentage of initial (construction) damages

$$d_h = \frac{h_1}{h_{tot}} \tag{13.b}$$

Table 3 resumes all the calculated damage indices. The influence of construction damages of the elements to the conformation of the axial load versus axial deformation diagram is presented in Fig. 11. As expected the percentage of damage (construction) affects the value of the maximum axial load and the corresponding strain (B-$D_mR_cR_j$-3, B-$D_mR_cR_jD_b$-4, B-$D_mR_cR_jD_b$-5 and A-$D_mR_cR_jD_b$-2) comparing to the values of load and strain of an undamaged specimen (R_c-1).

Figs. 12, 13 and 14 show the maximum normalized axial load of core versus the percentage of the damage of the section d_s, the percentage of the damage of the height d_h and the equal damage d_v respectively. The maximum load is normalized to the total section (A_c=150x150mm) and to the nominal concrete strength of the core f_c according to equation (Eq. (13.d))

$$n = \frac{P}{A_c \cdot f_c} \tag{13.d}$$

Section damage index (d_s) and height damage index (d_h) show dispersion and testify the need of the combination of the two indices to the d_v index in order to predict the resistance load accurately, which is also confirmed from Fig. 14. The correlation though, is quite satisfactory.

Also, Fig. 14 shows that the repaired cores present lower resistance load than the ones without damages which mean that the damage was not fully repaired. Also, minor damages are not necessarily effectively repaired.

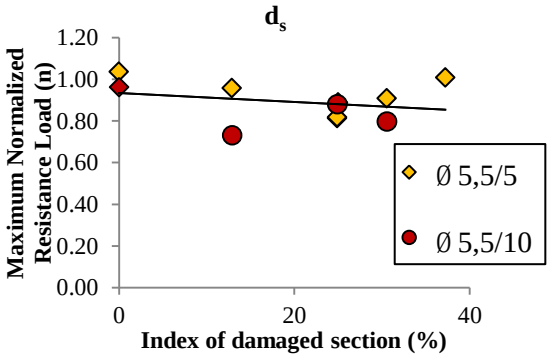

Fig. 12 Maximum normalized resistance load versus section damage index (n-d_s) after repair

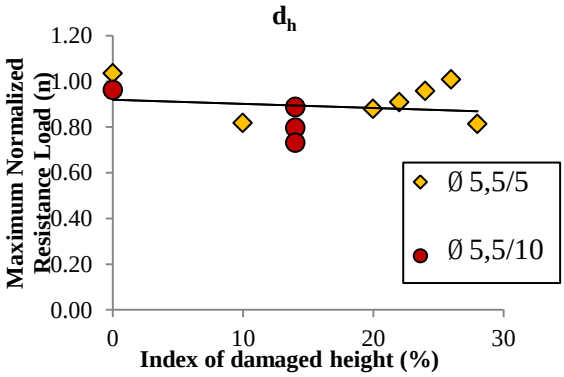

Fig. 13 Maximum normalized resistance load versus height damage index (n-d_h) after repair

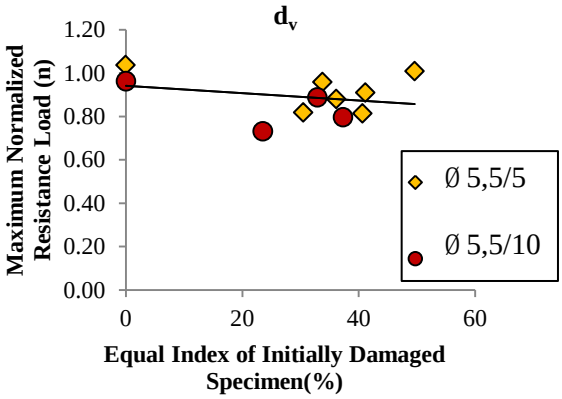

Fig. 14 Maximum normalized resistance load versus damage index (n-d_v) after repair

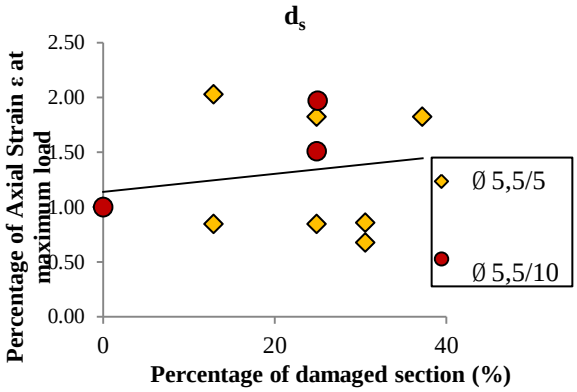

Fig. 15 Percentage of axial strain at maximum load versus section damage index (ε-d_s) after repair

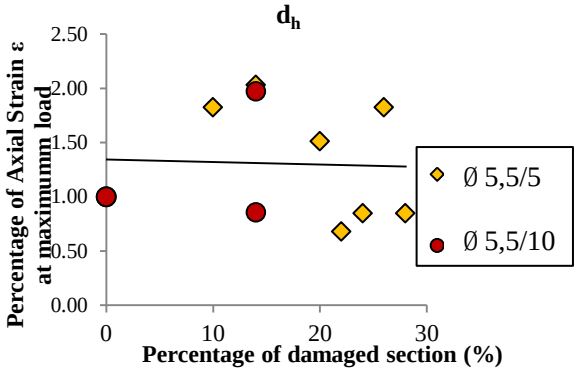

Fig. 16 Percentage of axial strain at maximum load versus height damage index (ε-d_h) after repair

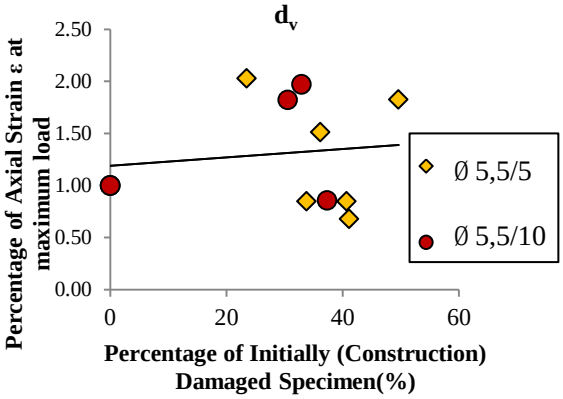

Fig. 17 Percentage of axial strain at maximum load versus damage index (ε-d_v) after repair

Specimens with construction damages and low mechanical percentage of stirrups (ω_{wc}=0.075), seem not to be suitably repaired. The specimen with the lowest damage (D_mR_c-3, d_v=24%) had the

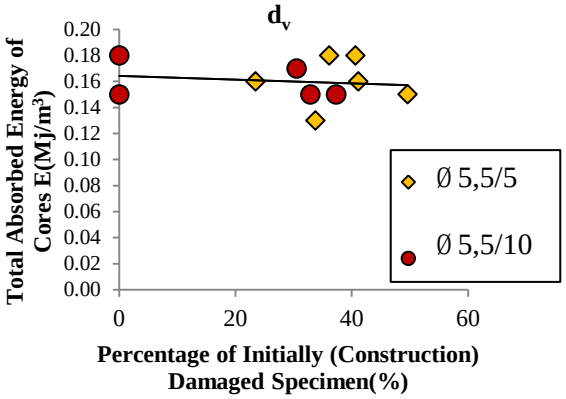

Fig. 18 Total absorbed energy of cores versus damage index (E-d_v) after repair

Table 4 Experimental results

Specimen	R.C. CORE (pre-loading)					R.C. JACKETED			
	δ_{peak} (P_{max}) (mm)	δ_u (P_u=20%P_{max}) (mm)	P_{max} (KN)	E_n (MJ/m³)	Load Case	δ_{peak} (P_{max}) (mm)	δ_u (P_u=20%P_{max}) (mm)	P_{max} (KN)	E_n (MJ/m³)
UR-1	6.30	7.60	563.15	0.10	-	-	-	-	-
R_c-1	4.50	4.80	613.40	0.15	-	-	-	-	-
D_mR_c-1	7.00	12.00	448.69	0.17	-	-	-	-	-
R_c-2	7.60	10.00	523.66	0.15	-	-	-	-	-
D_mR_c-3	6.90	10.00	487.08	0.15	-	-	-	-	-
D_mRc-4	7.10	12.00	401.20	0.16	-	-	-	-	-
D_mRc-5	7.00	10.00	553.29	0.15	-	-	-	-	-
A-UR-2	-	-	-	-	A	1.67	2.90	374.84	0.08
A-$D_mR_cR_jD_b$-1	5.80	11.00	482073	0.18	A	1.86	70.38	897.27	3.45
A-$D_mR_cR_jD_b$-2	3.00	5.45	436.97	0.15	A	1.50	62.00	782.21	2.20
A-$R_cR_jD_b$-3	6.40	6.60	528.59	0.09	A	1.32	72.41	452.63	2.07
A-$R_cR_jD_b$-4	-	-	-	-	A	2.03	63.19	198.77	0.18
A-$R_cR_jD_b$-5	-	-	-	-	A	2.28	62.89	370.05	0.36
B-$R_cR_jD_b$-1	-	-	-	-	B	1.92	45.01	633.03	1.45
B-$R_cR_jD_b$-2	3.25	4.92	525.49	0.13	B	3.78	52.23	814.22	1.79
B-$D_mR_cR_j$-3	3.90	5.45	441.90	0.18	B	6.52	50.95	1062.98	2.90
B-$D_mR_cR_jD_b$-4	2.60	4.45	498.45	0.16	B	4.39	49.23	942.43	2.14
B-$D_mR_cR_jD_b$-5	3.50	3.50	532.70	0.10	B	4.73	43.38	922.33	2.14
B-$R_cR_jD_b$-6	3.50	3.50	533.00	0.13	B	2.50	44.60	876.38	1.90
B-$R_cR_jD_b$-7	-	-	-	-	B	2.86	45.00	518.91	1.40
B-UR-3	-	-	-	-	B	1.68	5.39	810.30	0.05
B-URD_b-4	-	-	-	-	B	2.41	10.10	540.67	0.16

biggest reduced axial capacity (23%) of all other damaged columns. Though, specimens with more dense stirrups (ω_{wc}=0.15) testify that the gaps, created by the higher percentages of damage, when filled with material of high strength, the levels of reduction of the axial load capacity are lower. Specimen with the highest damage (D_mR_c-5, d_v=50%) presented only 10% reduction of axial load.

From all above results it is evident that the efficiency of the restoration/ repair depends strongly on the volumetric percentage of the existing transverse reinforcement.

Figs. 15, 16 and 17 show high dispersion between damage index d_v, d_s, d_h and the percentage of axial strain at maximum load ε (percentage to the ones without damages) is not sufficient. Moreover, Fig. 18, shows the total absorbed energy of cores versus the damage index d_v and

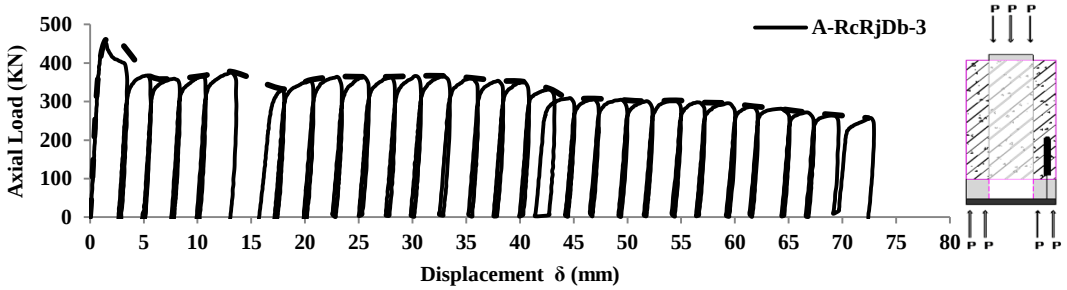

Fig. 19 Displacement versus Axial Load for A-$R_cR_jD_b$-3 (Load Pattern A)

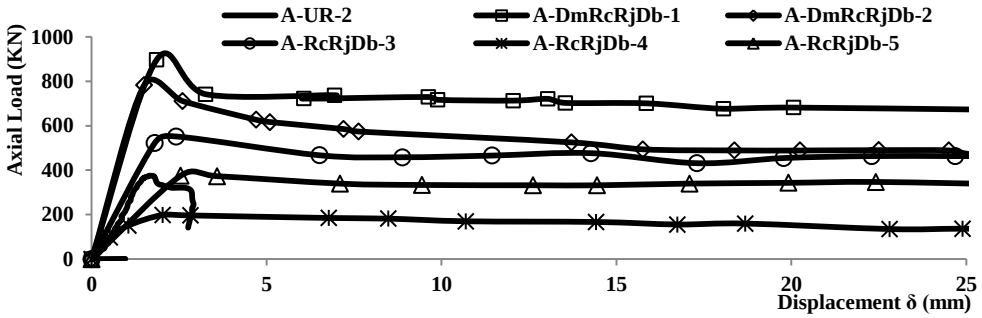

Fig. 20 Displacement versus Axial load for load pattern A (Envelopes)

presents again non-reliable correlation between those quantities. To result, damage indices d_v, d_h and ds do not provide information about the behaviour of the damages core after repair in terms of axial strain. More precisely, axial strain doesn't seem to be strongly affected from damage due to the fact that the confined area is not extensively damaged and helps the specimens to deform.

4.2 Load pattern results

Table 4 shows the results of each Load Pattern and the specimens tested respectively. Also the envelopes of the results of the cyclic test are shown in Fig. 18 to 28. It is noted that in Load Pattern A and B the columns were tested in high levels of axial displacements that are not feasible to the real structures in order to investigate the load transfer mechanisms. Table 6, though, includes the measured quantities: δ_{peak} is the displacement that corresponds to the maximum load (P_{max} also included), δ_u is the displacement corresponding to the ultimate load (δ_u>25mm, P_u=20%Pmax) and E_n is the total absorbed energy normalized to the volume of the core. All deformations are the relative displacements of the two loading plates at the top and bottom of the specimens as shown in Fig. 9. For the Load Pattern A the deformation is equal to slip between core and jacket.

In Load Pattern A, that examines the transfer mechanisms (Figs. 19, 20) specimen without initial construction damages (A-$R_cR_jD_b$-3, ω_{wc}=0.075 ω_{wj}=0.46), with no interface treatment presented 14% lower capacity than it's capacity to compression before jacketing (pre-loading effect).

Specimens with initial construction damages (A-$D_mR_cR_jD_b$-1: ω_{wc}=0.15 ω_{wj}=1.86 d_v=36%, A-$D_mR_cR_jD_b$-2: ω_{wc}=0.075 ω_{wj}=0.92 d_v=36%) presented higher maximum load (50% and 42%

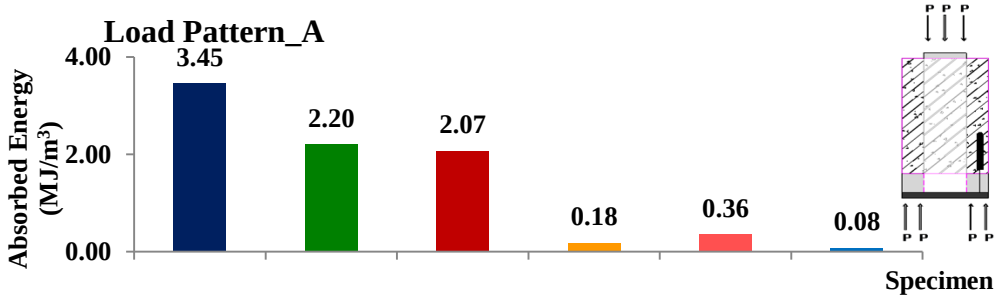

Fig. 21 Absorbed energy up to failure for load pattern A

Fig. 22 Cut of jacketed specimen A-$D_mR_cR_jD_b$-1 after loading- dowel deformation

Fig. 23 Jacketed specimen A-$D_mR_cR_jD_b$-1 after failure of stirrups

respectively) than the undamaged specimen (A-$R_cR_jD_b$-3) in higher values of slip (30% and 12% respectively). That testifies that the treatment of the interface helped favorably the maximum load capacity and the resistance of the interface to slip.

Also, the specimen with the maximum percentages of stirrups in core and jacket (A-$D_mR_cR_jD_b$-1: ω_{wc}=0.15 ω_{wj}=1.86) presented the maximum load of all, proving that the confinement mechanisms were activated and contributed in terms of load and slip.

The absence of cohesion and friction in specimens coated with polymer sheets (A-$R_cR_jD_b$-4, A-$R_cR_jD_b$-5) helps to examine clearly the influence of dowels. Specimen with six dowels of 14mm diameter (A-$R_cR_jD_b$-4) presented 85% higher maximum load in 12% higher slip than specimen with six dowels of 10mm diameter (A-$R_cR_jD_b$-5). This confirms that the bigger the dowel diameter is, the higher the maximum bearing load is.

The unreinforced specimen (A-UR-2) was tested in order to define the cohesion and friction of plain concrete. It is noted that the maximum bearing load happened in values of slip (1.32mm-2.03mm) in which cohesion is considered to be lost.

The energy absorbed diagrams (Fig. 21) show that the total absorbed energy in columns with all shear mechanisms in action (A-$D_mR_cR_jD_b$-1, A-$D_mR_cR_jD_b$-2, A-$R_cR_jD_b$-3) cannot be calculated proportionally or simplified by adding the energy absorbed by each mechanism separately. Also, the dowel action does not contribute importantly at the total energy absorbed.

Fig. 22 shows a cut of the specimen A-$D_mR_cR_jD_b$-1 after loading and in Fig. 23 is shown the failure of the stirrups at the end of loading.

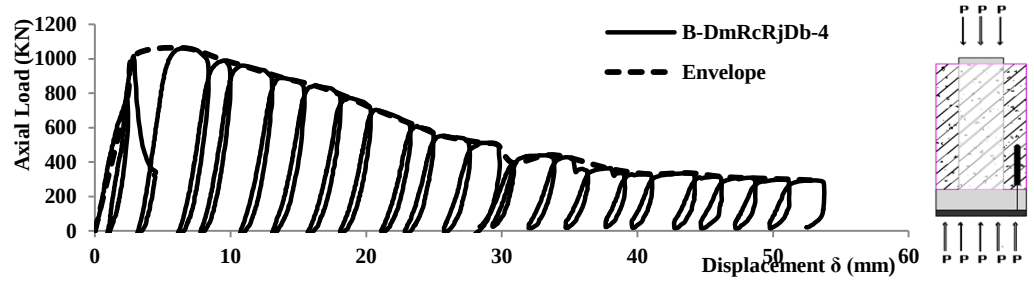

Fig. 24 Displacement versus Axial load for specimen B-$D_mR_cR_jD_b$-4 (load pattern B)

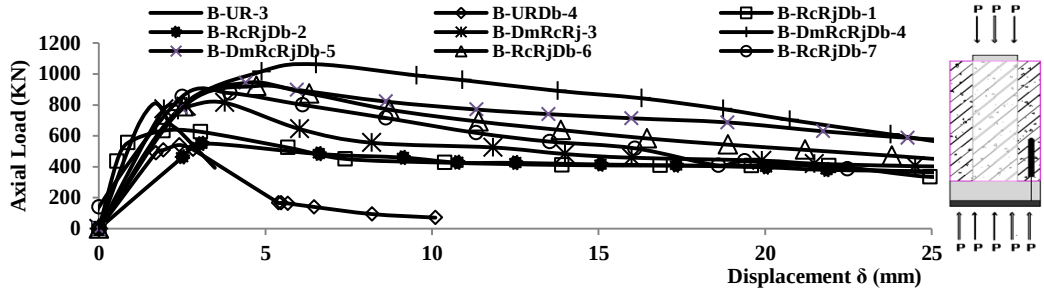

Fig. 25 Displacement versus Axial load for load pattern B (envelopes)

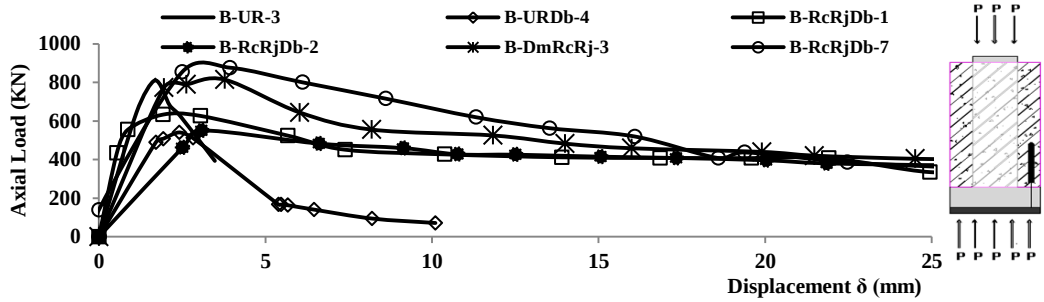

Fig. 26 Displacement versus Axial load-influence of Dowel action

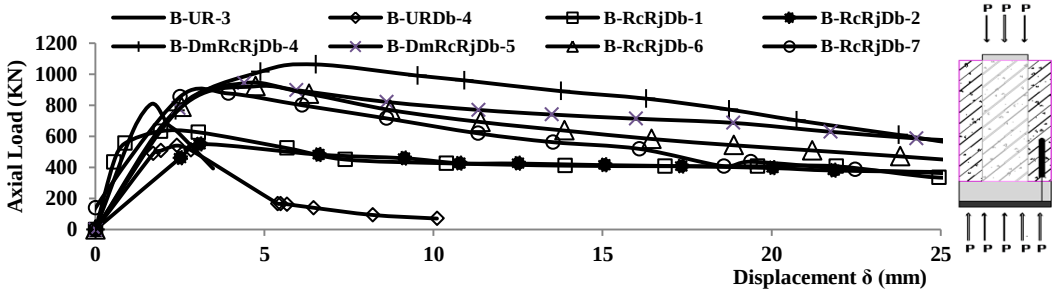

Fig. 27 Influence of jacket confinement to bearing capacity

In Load Pattern B which simulates a retrofitted column in real structures, (Figs. 24, 25) specimen containing dowels (B-$D_mR_cR_jD_b$-7: ω_{wj}=0.4) presented 7% higher load at 34% lower slip than specimen with no dowels (B-$D_mR_cR_j$-3: ω_{wj}=0.4). Though, specimen only with dowels crossing the interface (B-URD_b-4) proves that their presence affects the maximum load in small levels but increases the resistance of the interface to slip.

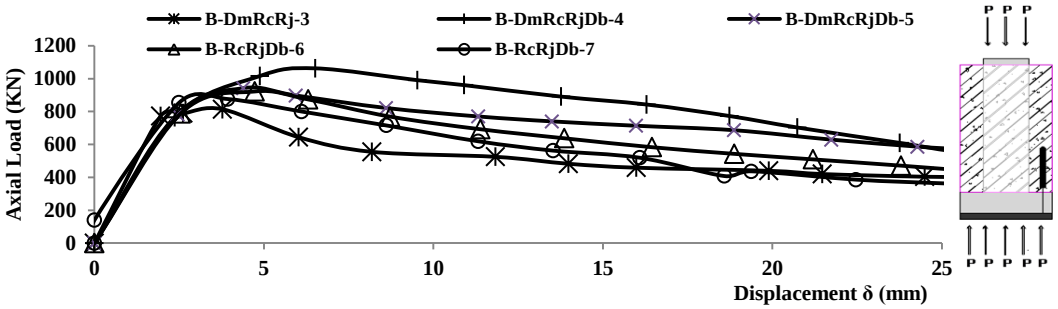

Fig. 28 Influence of initial damage to the effectiveness of the retrofitted column

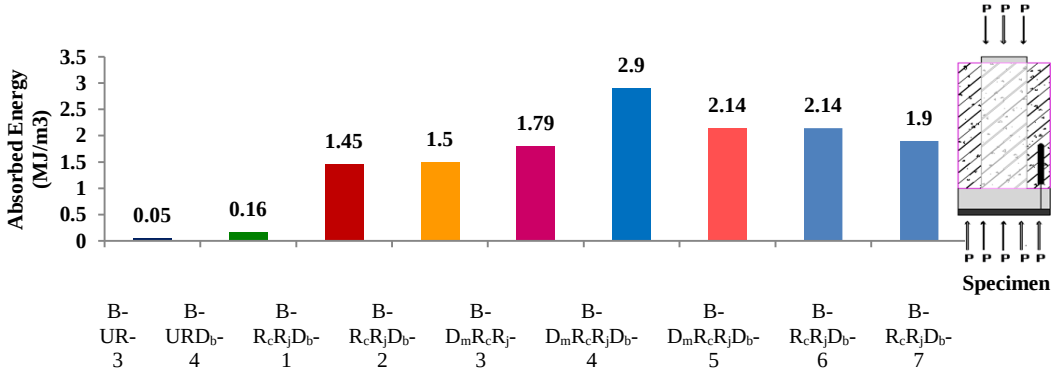

Fig. 29 Absorbed energy up to failure for load pattern B

The influence of the diameter of dowels is again examined by the columns covered with polymer sheets. Dowels of larger diameter (B-$R_cR_jD_b$-1, 6Ø 14) presented 28% higher maximum load at 96% lower values of slip than smaller diameters (B-$R_cR_jD_b$-2, 6Ø 10). It is noted that specimen with no reinforcement at all (B-UR-3) presents higher load than an unreinforced column with dowels crossing the interface (B-URD$_b$-4). The strong difference between those specimens is the actual mechanism of failure. The unreinforced column works only with tensile strength of the weakest concrete. The presence of dowels, on the other hand, creates damaged regions around the dowel bar that augment throughout the loading and the make the failure easier to expand. The influence of dowels is shown in Fig. 26.

The mechanical percentages of stirrups in the jacket area affect the maximum bearing load, as shown in Fig. 27. Specimens with dense stirrups presented the highest axial load capacity, proving again the activation of the confinement mechanisms.

Columns with construction damages (B-$D_mR_cR_j$-3, B-$D_mR_cR_jD_b$-4, B-$D_mR_cR_jD_b$-5) presented the highest maximum load of all tested columns in this Load Pattern. In fact, their resistance load exceeds the one they beard at the pre-loading tests, proving that the repair was effective (Fig. 28).

All above are also confirmed by the energy absorbed diagram (Fig. 29). The repair of the damaged columns was effective since there is no difference at the total absorbed energy comparing with an undamaged element (B-$D_mR_cR_jD_b$-5, B-$R_cR_jD_b$-6). The activation of confinement is also obvious specimen with the high percentage of stirrups absorbed the most energy (B-$D_mR_cR_jD_b$-4: ω_{wj}=1.86). Finally, again, the energy of the dowel action or cohesion alone or even in combination (B-UR-3, B- URD$_b$-4, B-$R_cR_jD_b$-1, B-$R_cR_jD_b$-2,) range in lower values.

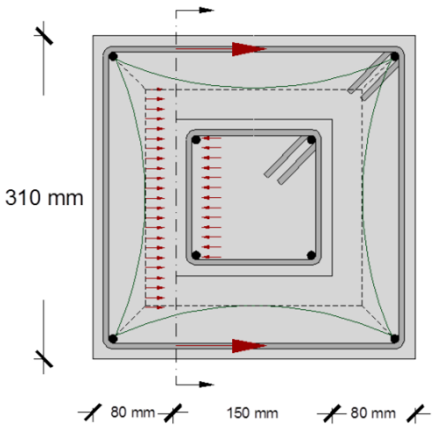

Fig. 30 Section of specimen

It is important to note that the values of the bearing load of Load Pattern A are similar to those of Load Pattern B. this means, that in Load Pattern B the forces are totally transferred to the jacket area.

4.3 Analytical results

In order to apply the relations of the codes, there is a need of defining the normal stress applied to the interface of the jacketed column. The stresses applied at the interface are the ones due to the expansion of the core concrete and the activation of the stirrups attributed to the clamping action of stirrup legs normal to the interface (Fig. 30). So, the stirrups develop their capacity to tension. In this way, the stresses applied by the stirrups to the interface are equal to the normal stress applied by the (mean) expansion of the core (Eq. (14)).

$$\sigma_0 = \frac{n_s \cdot 2 \cdot F_s}{A_{int}} \tag{14}$$

where:

n_s: is the number of the stirrups placed at the column (jacket)

F_s: is the force of the stirrups applied

A_{int}: is the area of the interface between core and jacket

In the following calculations steel is considered to function at the yield stress (the stirrups are considered to be in yield), as an upper limit for the calculations. The yield stress of the bars is extracted after tension tests and is calculated 250.76 MPa. Normally, the mean expansion of the core concrete should be expected as an upper limit 20% of the axial stress (if a Poisson's ratio of ν=0.2 is considered).

The values of σ_0 according to Eq. (14) are shown in Table 5.

The FIB code requires the axial and the normalized axial load applied at the column. The analytical results are all calculated with the maximum compression load that the retrofitted columns can stand. That is

$$N_{max} = N_c = A_s \cdot f_{yk} + A_{c,j} \cdot f_{ck,j} + A_{c,c} \cdot f_{ck,c} \tag{15}$$

Table 5 Total forces according to different codes- analytical results (6 dowels of 10mm diameter and nominal concrete strength f_c=24,37 MPa)

	ω_{wj}	σ_0		F_c		F_μ (KN)				F_d (KN)				F_{tot} (KN)			
FIB (Model Code 2010, bulletin 55)		**LPA**	**LPB**	**LPA**	**LPB**	**Lower limit**		**Upper limit**		**Lower limit**		**Upper limit**		**Lower limit**		**Upper limit**	
						LPA	**LPB**	**LPA**	**LPB**	**LPA**	**LPB**	**LPA**	**LPB**	**LPA**	**LPB**	**LPA**	**LPB**
	0.035	1.27	0.61	-	-	190.64		266.90		50.24		35.53		304.99		438.75	
	0.071	1.75	0.85	-	-	262.14		366.99		50.24		35.53		376.48		538.33	
	0.142	3.35	1.61	-	-	500.44		700.62		50.24		35.53		614.78		871.96	
						LPA		**LPB**		**LPA**		**LPB**		**LPA**		**LPB**	
ACI-318R-08 Building Code	0.035	1.27	0.61	-	-	266.90				118.17				385.07			
	0.071	1.75	0.85	-	-	366.90				118.17				485.16			
	0.142	3.35	1.61	-	-	700.62				118.17				818.79			
						LPA		**LPB**		**LPA**		**LPB**		**LPA**		**LPB**	
EN1998-3 (Greek Retrofit Code)	0.035	1.27	0.61	189.13	390.86	152.51				74.76				461.71		663.45	
	0.071	1.75	0.85	189.13	390.86	189.13				74.76				518.91		720.64	
	0.142	3.35	1.61	189.13	390.86	400.35				74.76				709.55		911.29	

$$n = \frac{N_{max}}{A_{c,j} \cdot f_{c,j} + A_{c,c} \cdot f_{c,c}} \quad (16)$$

Where:

A_s : area of the longitudinal bars

f_{yk}: yield stress of the longitudinal bars, as measured at the tension tests

$A_{c,c}$, $A_{c,j}$: area of the core and the jacket respectively

$f_{ck,c}$, $f_{ck,j}$: compressive strength of the core concrete and the jacket concrete, as measured at the compression tests

As a result, the maximum compressive load equals: N_{max}=2900.22 KN and the normalized axial load n=1.

The total forces applied at the interfaces of the columns are depicted according to the mechanical percentages of the stirrups of the jacket (ω_{wj}) and the diameter of the six dowels crossing the interfaces (Table 5).

Where:

F_c: the total force (four interfaces) due to cohesion

F_μ: the total force (four interfaces) due to friction

F_d: the total forced of the (six) dowels

F_{tot}: the total forces applied due to all above mechanisms

4.4 Comparison of experimental and analytical results

The provisions of *FIB* (Model Code 20120), ACI- 318R-08 Building Code, EN 1998 part 3-GRC in contradistinction with the experimental results in terms of maximum bearing load are shown in Table 6. In tests conducted to examine the interface alone (Load Pattern A) appeared values of axial load close to codes' provisions. More extensively, comparing experimental results with codes' values, at the absence of cohesion and friction, ACI, EN 1998 part 3- GRC and the lowest limit of *FIB* seem to converge to the same values depending on the diameter of dowels. The upper limit of *FIB* is 16% and 10% lower than the experimental results for dowels of 10mm and 14mm diameter respectively (A-$R_cR_jD_b$-4, A-$R_cR_jD_b$-5). For larger diameters codes seem to be conservative. Additionally, the influence of confinement is remarkable in each code. For different

Table 6 Experimental & analytical results for the tested specimens

Specimen	Experimental Results		Codes Provisions			
			FIB (Model Code 2010,bulletin 55)		ACI-318R-08 Building Code (KN)	EN1998-3 (Greek Retrofit Code) (KN)
	δ_{peak} (P_{max}) (mm)	P_{max} (KN)	Lower Limit (KN)	Upper Limit (KN)		
A-UR-2	1.67	374.84	-	-	-	189.13
A-$D_m$$R_c$$R_j$$D_b$-1	1.86	897.27	614.78	871.96	700.62	709.55
A-$D_m$$R_c$$R_j$$D_b$-2	1.50	782.21	376.48	538.33	485.16	518.91
A-$R_c$$R_j$$D_b$-3	1.32	452.63	304.99	438.75	385.07	461.71
A-$R_c$$R_j$$D_b$-4	2.03	198.77	114.34	171.34	118.17	120.07
A-$R_c$$R_j$$D_b$-5	2.28	370.05	224.11	335.83	231.61	235.34
B-$R_c$$R_j$$D_b$-1	1.92	633.03	115.80	162.13	231.61	235.34
B-$R_c$$R_j$$D_b$-2	3.78	814.22	59.08	82.72	118.17	120.07
B-$D_m$$R_c$$R_j$-3	6.52	1062.98	190.64	266.90	266.90	341.64
B-$D_m$$R_c$$R_j$$D_b$-4	4.39	942.43	614.78	871.96	818.79	911.29
B-$D_m$$R_c$$R_j$$D_b$-5	4.73	922.33	376.48	538.33	485.16	911.29
B-$R_c$$R_j$$D_b$-6	2.50	876.38	376.48	538.33	485.16	911.29
B-$R_c$$R_j$$D_b$-7	2.86	518.91	304.99	438.75	385.07	663.45
B-UR-3	2.41	540.67	-	-	-	390.86
B-URD_b-4	1.68	810.30	114.34	171.34	118.17	510.93

percentages of confinement of the jacket the provision of ACI, EN 1998 part 3- GRC and the upper limit of *FIB* alternates due to the way codes consider friction (through friction coefficient), which is caused by the normal stress due to the clamping function of stirrups. What is more, it is concluded that all these mechanisms act and contribute to the elements' behaviour in values of experimental slip, always higher than the provisions' slip for each mechanism separately (Table 1). Load Pattern B confirms all above, proving that in real structures were loading is diffused form the old column and ends to the retrofitted section, all these mechanisms act in the same way.

5. Conclusions

The present study focuses on the effect of the initial damages of core to the final bearing load of the jacketed column. Due to initial (construction) damages the loading capacity is decreased and the deformation ability is affected. Suitable repair of damaged core can lead to increased maximum transferred load through the interfaces. The different Load Patterns demonstrate the variable activation of the transverse reinforcement of the jacket and the dowel action. These factors contribute to maximum bearing load as well as to the resistance of the interface to slip. What is more, in both Load Patterns the load is transferred to the jacket are in the same way. Initial construction damages reduce the ability of the element to act as monolithic even when suitably repaired. Though, the more extensive is the damage and the repair of it, the better is the final behaviour of the column. As a result, an accurate model is required to quantify and predict the behaviour of the jacketed column in terms of damages, load capacity and deformation in order to be incorporated into codes.

Acknowledgements

The authors wish to thank Sika Hellas for providing the resins.

References

Fardis, M.N. (2009), *Seismic Design, assessment and retrofitting of concrete buildings, based on EN-Eurocode 8, Geotechnical, geological and earthquake engineering,* Springer.

Julio, N.B.E., Branco, A.B.F. and Silve, D.V. (2005), "Reinforced concrete jacketing- interface influence on monotonic loading response", *ACI Structural Journal*, **102**(2), 252-257.

Haskett, M., Oehlers, D.J., Mohamed Ali, M.S. and Sharma, S.K. (2011), "Evaluating the shear-friction resistance across sliding planes in concrete", *Engineering Structures*, **33**(4), 1357-1364.

Ince, R., Yalcin, E. and Arslan, A. (2007), "Size-dependent response of dowel action in R.C. members", *Engineering Structures*, **29**(6), 955-961.

Sim, J.I., Yang, K.H. and Jeon, J.K. (2013), "Influence of aggregate size on the compressive size effect according to different concrete types", *Construction and Building Materials*, **44**, 716-725.

Xiao, J.Z., Xie, H. and Yang, J.Z. (2012), "Shear transfer across a crack in recycled aggregate concrete", *Cement and Concrete Research*, **42**(5), 700-709.

Spathis, A.L., Bousias, N.E. and Fardis, N.M. (2006), "Tests of reinforced concrete columns retrofitted with reinfirced concrete or FRP jackets", *15th Concrete Conference* ,Technical Chamber of Greece, Alexandroupolis. (in Greek)

Vandoros, G.K. and Dritsos, E.S. (2006a), "Concrete jacket construction detail effectiveness when strengthening RC columns", *Constructona and Building Materials*, **22**, 264-276.

Vandoros, G.K. and Dritsos, E.S. (2006b), "Axial preloading effects when reinforced concrete columns are strengthened by concrete jackets**",** *Prog. Structural Eng. Mater.*, 79-92.

Thermou, G.E., Papanikolaou, V.K. and Kappos, A.J. (2011), "Analytical model for predicting the response of old type columns rehabilitated with concrete jacketing under reversed cyclic loading", *COMPDYN 2011 III ECCOMAS, Thematic Conference on Computational Methods in Structural Dynamics and Earthquake Engineering Corfu*, Greece.

International Federation for Structural Concrete (2010), "First Complete Draft", *fib-Model Code 2010, bulletin 55.*

American Concrete Institute (2008), "Building Code Requirements for Structural Concrete (ACI 318-08) and Commentary", *ACI -318R-08 Building Code.*

European Standard EN (2005), "Eurocode 8 design of structures for earthquake resistance, Part 3: Assessment and retrofitting of buildings".

Organisation of Seismic Design and Protection (2012), "Greek Retrofit Code". (in Greek)

Achillopoulou, D.V., Rousakis, T.C. and Karabinis, I.A. (2012), "Force transfer between existing concrete columns with reinforced concrete jackets subjected to pseudoseismic axial loading", *Proceeding of 15th WCEE*, Lisbon.

List of symbols

A_c	:	Section area (mm^2)
$A_{c,c}$	:	Area of core section (mm^2)
$A_{c,j}$	:	Area of jacket section (mm^2)
A_{int}	:	Area of interface between core and jacket (mm^2)
A_s	:	Total reinforcement crossing the interface (mm^2)
A_{vf}	:	Clamping reinforcement (mm^2)
$\cos\alpha$	:	Cosine of the angle between shear friction reinforcement and shear plane
d_{AGR}	:	Maximum diameter of aggregates (mm)

d_b : Diameter of one dowel bar (mm)
d_h : Damage index axially (mm)
d_s : Section damage index (%)
d_v : Damage indicator (%)
E_c : Modulus of elasticity (GPa)
E_n : Total absorbed energy normalized at the volume of the core (MJ/m^3)
f_1 : Area of damage of the section (mm^2)
F_c : Total force due to cohesion (KN)
f_{cc} : Compressive strength of concrete under uniaxial stress (MPa)
f_{cd} : Nominal compression stress of concrete (MPa)
$f_{ck,c}$: Compressive stress of core's concrete (MPa)
$f_{ck,j}$: Compressive stress of jacket's concrete (MPa)
f_{ct} : Tensile strength of concrete
F_d : Total force of dowels (KN)
F_s : Force of one dowel bar
F_s : Force of stirrups (KN)
f_{tot} : Total area of section (mm2)
F_{tot} : Total force due to all shear mechanisms (KN)
F_{ud} : Ultimate dowel force (KN)
f_y : Tension yield stress of non- prestressing reinforcement (MPa)
f_{yd} : Nominal yield stress of steel (MPa)
F_μ : Total force due to friction (KN)
h_1 : Length of the damage axially (mm)
h_{tot} : Total length of the column (mm)
k : Coefficient of section (fib bulletin 55)
LPA : Load Pattern A
LPB : Load Pattern B
n : Normalized axial load
N_{max} : Maximum compression load of the retrofitted element (KN)
ns : Number of stirrups included in the jacket
P : Maximum load (KN)
P_{max} : Maximum bearing load (KN)
Pu : 20% of maximum load (KN)
s : Slip of interface
s : slip (relative displacement of steel and concrete cross-sections), shear slip (at interfaces) (mm)
s_{fu} : Slip beyond which friction is lost (EN1998-part3-GRC)
$\sin\alpha$: Sine of the angle between shear friction reinforcement and shear plane
s_{max} : is slip when F0,max is reached (mm)
V_n : Nominal shear strength (KN)
δ_{peak} : Deformation corresponding to the maximum load (mm)
δ_u : Deformation corresponding to 20% of maximum load (mm)
$\varepsilon_{\rho l,l}$: Axial strain corresponding to the 85% of the maximum load (pre-loading)
$\varepsilon_{\rho l,max}$: Maximum axial strain of monotonic pre-loading
κ : Interaction "effectiveness" coefficient
λ : Coefficient (ACI-318R-08)
μ : Friction coefficient
ρ : Ratio of reinforcement of the interface
σ_0 : Normal stress of the interface
σ_0 : Normal stress applied at the interface due to expansion of the core (MPa)
σ_{cd} : Normal stress applied at the interface
τ : Shear stress

ω_{wc} : Mechanical percentage of transverse reinforcement of core
ω_{wj} : Mechanical percentage of transverse reinforcement of jacket